Section 1.3

Photometric Data, Magnitudes, and Variability

1.3. Photometric Data, Magnitudes and Variability

1.3.1. Hipparcos (Main Mission) Photometry: Single Stars

An introduction to the Hipparcos observations has been given in Section 1.1.1. The astrometric results contained in the Hipparcos Catalogue were derived from observations made at different epochs as the satellite scanned the celestial sphere. The modulated signal was measured by a photon-counting image dissector tube device. Whilst the phase of the modulated signal provided the astrometric information, its mean level and amplitude contained information on the intensity of the observed objects.

Both the mean level (dc component) and the amplitude (ac component) were used to produce fully calibrated magnitudes for each object at each epoch of observation. The dc component is the more powerful and precise measurement of the two, but is affected by background. The ac component is insensitive to the background level, but influenced by duplicity. The photometric data presented in the main Hipparcos Catalogue and in the Hipparcos Epoch Photometry Annex have been derived from the dc component. Corresponding results for the ac component can be found in the Hipparcos Epoch Photometry Annex Extension.

The Hipparcos main instrument observed in a broad-band system in order to optimise the astrometric signal. This system is referred to as Hp and is specific to the Hipparcos configuration (Figure 1.3.1). The photometry obtained with such a broad-band system is limited in its astrophysical content compared to multi-colour photoelectric photometry. The precision of each observation is, however, high.

The main mission photometric data were reduced using a selection of 22 000 standard stars. This list included some stars which could not be strictly regarded as photometric standards, in particular among the very red stars—these stars were nevertheless necessary for the control of the calibration parameters for stars with extremely red colour indices. An initial selection was made on the basis of ground-based photometry, using standard stars identified in the Hipparcos Input Catalogue. The final standard star list incorporates some new standard stars, while some stars from the initial selection were classified as variable on the basis of the Hipparcos measurements and subsequently rejected as standards.

The resulting collection of epoch photometry comprises a total of 13 000 000 observations, an average of some 110 observations for each of the 118 000 programme stars. While significant variations in the number of observations occurred, primarily related to the object's ecliptic latitude, the Hipparcos Epoch Photometry represents the largest compilation of high-precision, multi-epoch photometry acquired to date. It consequently defines a uniform all-sky photometric system, unaffected by seasonal and hemisphere-related influences.

The epoch photometry can be affected by a difference between the Cousins' $(V-I)_{\rm C}$ colour used in the reductions and the actual colour of the star, due to the ageing of the optical chain and the resulting changes in the passband. Section 1.3.4 includes a description of how the epoch photometry can be corrected for such colour errors.

1.3.2. Hipparcos (Main Mission) Photometry: Double Stars

The Hipparcos photometry for double and multiple stars had to be treated with particular care. The image dissector tube detector had an instantaneous field of view of about 30 arcsec diameter, attenuation starting at about 5 arcsec from the centre. For double stars with separations between 5 and 20 arcsec one or both of the components was therefore inevitably positioned where the attenuation of the instantaneous field of view changed rapidly. Observed intensities were therefore very sensitive to the exact pointing of the instantaneous field of view with respect to the stellar images. This was of importance in particular when the two components of a double star were of similar brightness. In many such cases the resulting photometric data were unreliable, and were accordingly flagged.

A total of 5803 entries for double stars had their dc magnitudes corrected for the effects of measuring off-centre in the instantaneous field of view, and for the presence of another component within the same instantaneous field of view. They are among 12 961 entries which can be recognised from the component flag in the first header record of the epoch photometry data file: if not blank, the star is a double star and significant corrections may have been applied. The largest corrections were made for stars with component flag 'B', followed by those with component flag 'A'. Corrections made for stars with component flag '*' were generally very small. All stars with the component flag set have the correction that was applied given in the header records of the Hipparcos Epoch Photometry Annex file. As ac magnitudes were not corrected, these stars should be excluded from investigations involving comparisons between ac and dc magnitudes. This section describes the corrections that were applied to double star photometry.

Every object in the Hipparcos Input Catalogue had its own target position, used by the satellite to point the sensitive area of the image dissector tube detector. For single stars this was simply the direction of the star. Double stars with separations below 10 arcsec were observed as a single catalogue entry, with the target position being either at the photocentre or at the geometric centre of the two components. Components of double stars with wider separations were considered as separate potential targets although not all components of such systems were necessarily included in the Hipparcos Input Catalogue. The pointing of the detector's instantaneous field of view had an associated uncertainty of a few arcsec, unimportant for single stars except for the very brightest. However, for double or multiple stars with at least one component near the steep slope of the detector's response profile, these uncertainties were important.

The typical situation is illustrated in Figure 1.4.1 of Section 1.4, and the detector's response profile is given in Table 1.4.1. The response was characterised by a flat region of about 5 arcsec in diameter (attenuation ≤ 0.01 mag) followed by a slow decline in sensitivity up to 11 arcsec (attenuation ~ 0.1 mag), and finally a sharp increase in attenuation at larger distances.

During the observations of a double star with a separation between 5 and 35 arcsec, pointing at the primary, the secondary was not always on the central part of the detector's profile and could consequently appear dimmed. The total intensity as measured by the instrument was therefore smaller than the true intensity. The photometric results for such double stars have been corrected for this effect, in the computation of both the combined magnitudes and the component magnitudes.

For the simplest case with the detector pointing at the primary, the intensity ratio between the primary and secondary is given by:

$$r = \frac{I_2}{I_1} = 10^{-0.4\,\Delta m} \qquad [1.3.1]$$

where Δm is the magnitude difference between the two components, and I_1, I_2 the corresponding intensities. For the instrumental magnitude difference, $\widetilde{\Delta m} = \Delta m + \psi(\varrho)$ where ϱ is the component separation, and $\psi(\varrho)$ is the attenuation profile expressed in magnitudes. This yields the instrumental intensity ratio:

$$\tilde{r} = \frac{\tilde{I}_2}{I_1} = 10^{-0.4\,\widetilde{\Delta m}} \qquad [1.3.2]$$

The combined true intensity is given by:

$$I = I_1 + I_2 = I_1(1 + r) \qquad [1.3.3]$$

while the measured quantity was:

$$\tilde{I} = I_1 + \tilde{I}_2 = I_1(1 + \tilde{r}) \qquad [1.3.4]$$

From which:

$$Hp = \tilde{H}p + 2.5 \log \frac{1 + \tilde{r}}{1 + r} \qquad [1.3.5]$$

and:

$$H_1 = \tilde{H}p + 2.5 \log(1 + \tilde{r}) \qquad [1.3.6]$$

$$H_2 = \tilde{H}p + 2.5 \log(1 + \tilde{r}) - 2.5 \log r \qquad [1.3.7]$$

where Hp is the true combined magnitude, $\tilde{H}p$ the observed value and H_1, H_2 the true magnitudes of the two components. Similar expressions apply for a pointing at the geometric centre, where simultaneous allowance is made for the attenuation of the primary and secondary components.

A correction has been applied to all the transits of the Hipparcos Epoch Photometry Annex of the double stars included in Part C of the Double and Multiple System Annex in order to derive the combined magnitude Hp, and the magnitudes of the components. No correction was applied to double stars not resolved by Hipparcos, and as a consequence no information is given for the component flag in Field HH2. The magnitude of the components of the triple and quadruple stars have been corrected by adapting Equations 1.3.5–1.3.7 to more than two components, but only for the summary photometric information given in the Double and Multiple Systems Annex. The errors on ϱ and Δm have been propagated and added quadratically to the estimated standard error of the Hp magnitude of the transits and to that of the median $\overline{Hp}$.

The corrections were computed in a uniform way assuming a pointing at the brighter component for each single-pointing system and at the brighter or fainter component for every two pointing system. While this is not perfectly rigorous for a system with the pointing at the geometric centre, the median of the resulting error is less than 1 millimagnitude over the 760 such systems and reaches a level of 0.02 mag only for about 10 systems with separation close to 10 arcsec and with components of nearly equal brightness. The choice made was motivated by the need to have a correction that was easily reversible. More detailed corrections were not justified, considering this error in comparison with other uncertainties affecting the photometry of the double stars, such as the typical standard error of Δm of several hundredths of mag, the unknown variability of the components, the fact that the colour has been taken as some mean colour for the system and, for systems with large separation, the instability of the signal due to pointing offset.

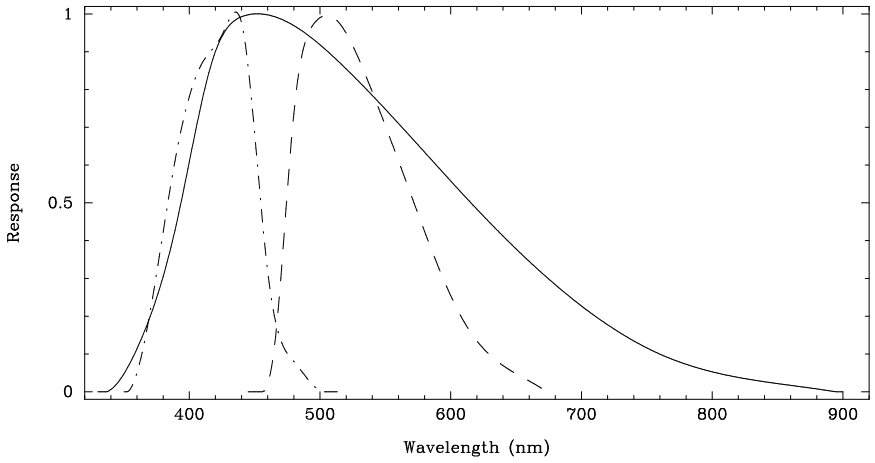

Figure 1.3.1. *The Hipparcos (Hp, solid line) and Tycho (B_T, dot-dash line, and V_T, long-dash line) photometric systems.*

Table 1.3.1. The Hp, V_T and B_T passbands as a function of wavelength (in nm).

λ	B_T	V_T	Hp	λ	B_T	V_T	Hp	λ	V_T	Hp	λ	Hp
330	0.000	0.000	0.000	475	0.101	0.530	0.979	620	0.135	0.483	765	0.092
335	0.000	0.000	0.000	480	0.080	0.737	0.969	625	0.114	0.465	770	0.085
340	0.000	0.000	0.006	485	0.059	0.870	0.958	630	0.097	0.447	775	0.079
345	0.000	0.000	0.023	490	0.036	0.940	0.946	635	0.082	0.429	780	0.073
350	0.000	0.000	0.047	495	0.016	0.973	0.933	640	0.069	0.412	785	0.067
355	0.014	0.000	0.078	500	0.003	0.990	0.919	645	0.058	0.395	790	0.062
360	0.058	0.000	0.114	505	0.000	0.996	0.903	650	0.047	0.378	795	0.057
365	0.123	0.000	0.154	510	0.000	0.991	0.888	655	0.038	0.361	800	0.053
370	0.206	0.000	0.198	515	0.000	0.975	0.871	660	0.028	0.345	805	0.049
375	0.305	0.000	0.248	520	0.000	0.949	0.855	665	0.018	0.329	810	0.045
380	0.416	0.000	0.305	525	0.000	0.916	0.838	670	0.008	0.314	815	0.041
385	0.530	0.000	0.369	530	0.000	0.878	0.820	675	0.000	0.298	820	0.038
390	0.636	0.000	0.442	535	0.000	0.837	0.803	680	0.000	0.283	825	0.035
395	0.724	0.000	0.523	540	0.000	0.794	0.785	685	0.000	0.269	830	0.032
400	0.787	0.000	0.608	545	0.000	0.749	0.766	690	0.000	0.254	835	0.029
405	0.830	0.000	0.694	550	0.000	0.704	0.748	695	0.000	0.241	840	0.026
410	0.861	0.000	0.774	555	0.000	0.658	0.729	700	0.000	0.227	845	0.024
415	0.889	0.000	0.845	560	0.000	0.612	0.710	705	0.000	0.214	850	0.022
420	0.920	0.000	0.901	565	0.000	0.565	0.691	710	0.000	0.201	855	0.019
425	0.953	0.000	0.941	570	0.000	0.518	0.672	715	0.000	0.189	860	0.017
430	0.982	0.000	0.967	575	0.000	0.471	0.653	720	0.000	0.177	865	0.015
435	1.002	0.000	0.984	580	0.000	0.424	0.634	725	0.000	0.166	870	0.012
440	0.976	0.000	0.993	585	0.000	0.379	0.615	730	0.000	0.155	875	0.010
445	0.861	0.000	0.998	590	0.000	0.335	0.596	735	0.000	0.144	880	0.007
450	0.685	0.000	1.000	595	0.000	0.293	0.577	740	0.000	0.134	885	0.005
455	0.489	0.000	1.000	600	0.000	0.254	0.558	745	0.000	0.125	890	0.002
460	0.317	0.022	0.998	605	0.000	0.218	0.539	750	0.000	0.116	895	0.000
465	0.202	0.115	0.993	610	0.000	0.186	0.520	755	0.000	0.108	900	0.000
470	0.136	0.301	0.987	615	0.000	0.159	0.502	760	0.000	0.100		

1.3.3. Tycho (Star Mapper) Photometry

In addition to the broad-band photometric observations acquired by the Hipparcos (main mission) detector, the star mapper data (which were processed independently and constitute the Tycho Catalogue) yielded two-colour photometric data, also at many different epochs. These two-colour observations correspond rather closely to (and can be approximately transformed into) the Johnson B and V magnitudes. The Tycho magnitude systems are referred to as B_T and V_T respectively. The spectral transmission (Figure 1.3.1 and Table 1.3.1) has been inferred from observations of photometric standard stars (updated with respect to ground-based calibrations of the instrument). The Tycho photometric data were reduced using standard stars which were initially selected on the basis of ground-based photometric standards identified in the Tycho Input Catalogue. The final standard star list included new standards, as well as the rejection of objects subsequently identified as variable.

The number of Tycho observations for each star is not given explicitly in the printed Hipparcos Catalogue. It is about 130 on average, dependent on ecliptic latitude as a result of the scanning law, and roughly 20–30 per cent larger than the number of Hipparcos photometric measurements of the same star (this number is given in the main catalogue). The larger number of observations of a given star by Tycho arises from the fact that, while the star mapper slits were only 40 arcmin in length, compared with the main field of view width of 54 arcmin, there were two slit groups.

The Tycho observations have a different spatial resolution compared with the Hipparcos observations—Tycho was able to distinguish directly components in double or multiple systems with separations $\varrho > 2$ arcsec. For such cases the B_T and V_T photometry might consequently refer to one or more components while the Hp photometry for the same catalogue entry may refer to the combined light from the system (even though the separate components may have been spatially resolved by Hipparcos). Similarly, duplicity can be recognised for some partly unresolved double stars from a relation between the observed magnitude and orientation of the slit group during the observation.

1.3.4. Photometric Data from Ground-Based Observations

The Hipparcos Input Catalogue included V magnitudes and $B-V$ colour indices obtained from ground-based observations, along with estimated Hp magnitudes, based on the pre-mission calculations of the Hp passband. During the mission, the Hp passband was re-calibrated as a function of wavelength and time, and Hp magnitudes were re-calculated based on the reconstructed passband at the 'photometric reference epoch' JD 2 448 622.5 (1 January 1992). This passband defines the Hipparcos broad-band photometric system, to which all observations have been reduced (see Volume 3).

The Cousins' $(V-I)_{\mathrm{C}}$ colour index was adopted as the colour parameter characterising the astrometric and photometric calibration of Hipparcos—it was appropriate for describing changes in the passband, being a more linear function of spectral type than $B-V$. In the photometric calibration it was used to describe the detector response as a function of location and star colour. This was time-dependent due to the chromatic ageing of the detector, principally as a result of radiation damage of the optical elements of the detection chain. In the astrometric calibration the $(V-I)_{\mathrm{C}}$ index was used to account for (small) chromatic effects. A specific effort was therefore devoted to the acquisition and compilation of the $(V-I)_{\mathrm{C}}$ colour indices, using a variety of ground-based observations as well as reduced Tycho data obtained over the first half of the mission. Although most of the Hipparcos and Tycho Catalogue data were derived exclusively from the satellite observations, the colour indices represent such an important piece of astrophysical information that they have been updated and included in the catalogue.

The Hipparcos Catalogue includes both $B-V$ (Johnson) and $V-I$ (Cousins) colour indices. The $B-V$ colour index was taken either from ground-based observations or from Tycho photometry when the latter was more accurate. Since the Tycho B_T, V_T and Johnson B, V bands differ, a straightforward linear transformation from B_T-V_T to $B-V$ may show residuals of up to 0.1 mag depending on star reddening, gravity, and temperature. Accurate transformations therefore utilised spectral type information, if available, and distinct transformation equations for dwarf and giant stars. Similarly, the $(V-I)_C$ indices were updated on the basis of the Tycho photometry and a variety of ground based data acquired during the post-launch phase. The source of the $B-V$ index is given in Field H39, the source of the $(V-I)_C$ index in Field H42. The transformations from Tycho data to $B-V$ and $(V-I)_C$ indices are described in Section 1.3 Appendix 4.

The Tycho Catalogue also includes $B-V$ colour indices, but derived only from the B_T-V_T values using the simplified transformation given in Section 1.3 Appendix 4, spectral type information not being available for a large fraction of the Tycho Catalogue entries. Consequently, the Tycho Catalogue $B-V$ colour indices are less accurate than those given in the Hipparcos Catalogue, and the two will frequently differ, for the same object, simply because they have been derived in different ways.

The requirement to preserve a record of the $(V-I)_C$ colour index used for the astrometric and photometric reductions, while at the same time presenting the best-available (updated) colour indices, meant that two catalogue fields are dedicated to $(V-I)_C$: Field H40 provides the best-available colour index at the time of the catalogue completion, while Field H75 (not included in the printed catalogue) provides the (intermediate) value used for the astrometric and photometric reductions. Re-reduction of the astrometric and photometric data would have been possible in principle, but unrealistic in practice: partly from the perspective of the catalogue completion schedule, but also because the 'final' $(V-I)_C$ (and the published $B-V$) values, still largely derived from a wide variety of ground-based observations, cannot be considered as definitive or fully homogeneous. However, in the case of the astrometric reductions the effect of an erroneous $(V-I)_C$ value was very small. Stars for which an erroneous $(V-I)_C$ is likely to have been used for the data reductions are indicated by R in Field H52.

The Hipparcos Epoch Photometry can be corrected for the effects of an erroneous $(V-I)_C$ colour index, used for the photometric reductions, once a new or improved colour index becomes available. The $(V-I)_C$ value used in the data reductions (Field H75) is transformed into a pseudo-colour, $C_{\rm old}$, according to the prescription given in Table 1.3.2. $C_{\rm new}$ is derived from the same table on the basis of the improved $(V-I)_C$ index. The correction $\delta Hp = Hp_{\rm old} - Hp_{\rm new}$ is then derived as:

$$\delta Hp = (0.0537\,(t-t_0) - 0.0084) \times (C_{\rm old} - C_{\rm new}) \qquad [1.3.8]$$

where t and t_0 are measured in units of 1000 Julian days, and t_0 = 2448.6225 =1 January 1992. The standard deviation of δHp when applying a colour correction of 1 mag is approximately 0.003 mag. This approximate correction applies only to dc magnitudes, and ignores small field of view differences. More accurate corrections using information from the Hipparcos Epoch Photometry Annex Extension are provided in Volume 3, Chapter 14, where corrections for the ac magnitudes are also given.

Table 1.3.2. Definition of the pseudo-colour index, $C = a + b(V-I) + c(V-I)^2 + d(V-I)^3$

Interval	a	b	c	d
$V-I \le 0.85$	−0.48729	0.98554	−0.31968	0.592
$0.85 < V-I \le 2.00$	−1.03936	2.14720	−0.416	0.0
$V-I > 2.00$	+0.5152	0.592	−0.0256	0.0

1.3.5. Published Data Related to the Hipparcos Photometry

The Hipparcos photometry has been presented in three ways: the fully reduced observations (the Hipparcos Epoch Photometry Annex plus Annex Extension), the results from a provisional variability search (the Variability Annexes and light curves) and summary data in the main Hipparcos Catalogue. The information contained in each of these products is summarised in the following sections. Full descriptions of formats and contents can be found in the relevant parts of Section 2.

The Hipparcos Epoch Photometry Annex: This annex provides the calibrated *Hp* epoch photometric data (based on the mean signal level, i.e. the dc magnitudes), along with an error estimate, quality flags and the barycentric time of each observation. The barycentric time is expressed in JD(TT) (see Section 1.2.3). The dc magnitudes have been provisionally corrected for 5803 stars in double systems, indicated by the component flag in the header record (see also Section 1.3.1 and Volume 3). Header records provide information on the number of observations, the $(V-I)_{\rm C}$ colour index used in the reductions, the median magnitude and its estimated error, the 5th and 95th percentiles (see Section 1.3 Appendix 1), and the variability indicator as defined in Section 1.3 Appendix 2. This information is repeated in the main Hipparcos Catalogue.

The Hipparcos Epoch Photometry Annex Extension: The extension provides data supplementary to the epoch photometry: the background levels used in the two reduction processes, the photometry based on the amplitude of the modulation (i.e. the ac magnitudes), the position on the sky in the complementary field of view, and an index for identified coinciding objects from the complementary field of view. These data allow for a more detailed and specialised analysis of the Hipparcos photometry. The header records partly repeat information from the headers in the Epoch Photometry Annex. Additional information related to the ac component is also provided. Information on the median ac magnitude and its estimated error has been used in the definition of the variability flag. The determination of the ageing corrections for the ac magnitudes were not as comprehensive as for the dc magnitudes, and small residual systematic effects may still be present.

Variability annex: tabular data and light curves: A provisional analysis of the photometric data referred to above was carried out in parallel by two distinct groups (at the Geneva Observatory and the Royal Greenwich Observatory). The tables of periodic and unsolved variables are the result of this analysis. Given the very limited time available, these classifications should not be considered as exhaustive or conclusive. The Hipparcos photometric data were examined with various period searching algorithms and results were compared with literature references when available. Period searches were severely handicapped by often very poor coverage of epochs by the observations, in particular for stars close to the ecliptic plane. The character of the scanning law made the recognition of periods in the range 5 to 100 days unreliable, in particular for semi-regular variables. Possible periods are given in the notes, but in most cases these periods are very likely to be spurious. Similarly, it was not always possible to distinguish between eclipsing binaries and pulsation- or rotation-related variations, leading to an ambiguity in the period given. Minimal time for proper classifications was available given the adopted catalogue publication schedule, and in many cases no classification could be provided.

The tabular data were split into two parts, corresponding to objects for which a variability period could be, or could not be, determined. For the 'periodic variables' the tabular material provides periods (given to the full estimated precision), amplitudes, reference epochs, variability types, star names, and references to the literature. The methods used for the period optimisation and the determination of the amplitude and its estimated error are described in Section 1.3 Appendix 3. Stars were also included in this table if the literature gave a reliable period and reference phase, but where these could not be independently derived using the Hipparcos data alone. This applies in particular to some long-period and Algol-type variables. In these cases no Hipparcos period is given, and sometimes also no Hipparcos reference epoch.

For the 'unsolved variables', amplitudes, variable star names, and references to the literature are also given. This table includes stars which were considered as semi-regular in the literature, but for which the period presented in the literature could not be confirmed by the Hipparcos data. In general, a star appearing in the table of unsolved variables is not necessarily non-periodic: it may only be concluded that a period was not established from this preliminary analysis, or confirmed from the literature.

All variables appearing in the table for the 'periodic variables', except those with very long periods, have their folded light curve given in Volume 12, Section A. For some of the more interesting stars (in this case the more slowly evolving) among the 'unsolved variables' the epoch photometry is shown graphically in Volume 12, Section C.

Prior to the start of the Hipparcos observations it was realised that for large-amplitude semi-periodic and irregular variables the Hipparcos photometry needed support from ground-based data. This was also essential in planning of the astrometric measurements: a proper optimisation of the observing time required *a priori* knowledge of the magnitude of every object. A selection of 296 large amplitude variables was monitored successfully by the AAVSO, and the Hipparcos data for these stars are shown superimposed on the fitted curves through the AAVSO data in Volume 12, Section B. Some of these stars appear in the table of 'periodic variables', in which case there will also be a folded light curve presented in Volume 12, Section A.

Summary photometric data in the Hipparcos Catalogue: The main Hipparcos Catalogue contains a summary of information extracted from, and provided in, the header records of the Hipparcos Epoch Photometry Annex and Annex Extension. Other information comes from the Variability Annexes, except for Field H6. A coarse variability flag is given in Field H6, derived from the distribution of unit weight residuals as described in Section 1.3 Appendix 2. It provides an estimate for intrinsic variability present in the epoch photometry under the assumption that the underlying variations are approximately sinusoidal. No provision for possible eclipsing binaries were made.

Fields H44–50 and H52 summarise the epoch photometry through medians, scatter estimates, and a simplified variability indicator, all as given in the header records in the Hipparcos Epoch Photometry Annex. Field H51 gives a period (to an accuracy of no more than 0.001 days) when this period has been derived solely from Hipparcos data. Fields H53–54 provide reference flags to the tabular data and light curves respectively.

1.3.6. Published Data Related to the Tycho Photometry

A similar approach was followed for the Tycho photometric results as for the Hipparcos photometric results. Thus, the Tycho Epoch Photometry Annex contains 'epoch photometry', and the main Tycho Catalogue contains summary data. The main differences are: (1) only a relatively small number of the Tycho Catalogue entries are retained with epoch photometry, because of the lower precision of the individual B_T and V_T magnitudes; (2) the summary statistics differ in some details: a 'de-censored mean' rather than a direct median is used, and different percentiles of the distribution are used to characterise the scatter; (3) a systematic variability analysis was not carried out for the Tycho Catalogue entries, so there is no corresponding 'variability annex'.

Summary data provided in the Tycho Catalogue: The Tycho Catalogue provides the median or mean magnitude and related statistics for each catalogue entry.

Estimates of the median or mean B_T and V_T magnitudes could not be simply constructed from the observed photometric transits. A meaningful median magnitude could only be derived from the Tycho observations for stars brighter than V_T ~ 8 mag and B_T ~ 8.5 mag. For fainter stars an increasing number of observations fell below the detection threshold, with the observations becoming critically signal-to-noise limited and the detection probability becoming a strong function of stellar magnitude and instantaneous background intensity. Ignoring the non-detections would have resulted in a biased sample of observations. In practice, fainter Tycho mean magnitudes have been obtained using a 'survival analysis' technique taking into account the non-detections, and are referred to as 'de-censored mean magnitudes'.

Compared with the Hipparcos Catalogue, where the 5th and 95th percentiles are used to represent minimum and maximum magnitudes, the 95th percentiles are not well-defined for many of the fainter Tycho stars (because of the censoring of observations); the 15th and 85th percentiles are therefore provided instead.

Estimates of the standard errors of the B_T and V_T magnitudes were also affected by the censoring of the fainter observations. Moreover, the standard errors in the Tycho Catalogue are much larger than in the main Hipparcos Catalogue, and the points equivalent to the 15th and 85th percentiles are not well centred on the de-censored mean values, because of the non-linear transformation between intensities and magnitudes. Consequently, Fields T33 and T35 of the Tycho Catalogue provide estimates of the standard errors specifically towards *brighter* magnitudes:

$$\begin{aligned} \bar{\sigma}_{B_T} &= \langle B_T \rangle - B_T(\langle I_{B_T} \rangle + \sigma_{I_{B_T}}) \\ \bar{\sigma}_{V_T} &= \langle V_T \rangle - V_T(\langle I_{V_T} \rangle + \sigma_{I_{V_T}}) \end{aligned} \qquad [1.3.9]$$

where $\langle I_{B_T} \rangle$ and $\langle I_{V_T} \rangle$ are the de-censored mean intensities with standard errors $\sigma_{I_{B_T}}$ and $\sigma_{I_{V_T}}$, as determined in the 'de-censoring analysis' (see the introduction to Section 2.2, and Section 2.2 Fields T32–39). Uncertainties towards fainter magnitudes are larger than those towards brighter magnitudes. The latter has been chosen for the definition of the standard error because it may always be computed (unlike that towards fainter magnitudes, which is infinite when the standard error is as large as 0.753 mag, i.e. $\sigma_I = I$). Further details are given in Volume 4, Chapter 9.

Similarly, the change in magnitude corresponding to a shift of intensity by $n\,\sigma_I$ is given by:

$$\begin{aligned} \Delta B_T(n\sigma_{I_{B_T}}) &= |2.5 \log(1 + n - n\, 10^{0.4\bar{\sigma}_{B_T}})| \\ \Delta V_T(n\sigma_{I_{V_T}}) &= |2.5 \log(1 + n - n\, 10^{0.4\bar{\sigma}_{V_T}})| \end{aligned} \qquad [1.3.10]$$

where n is negative towards brighter magnitudes and positive towards fainter magnitudes. Thus 1σ uncertainties towards fainter magnitudes are given by:

$$\begin{aligned} \sigma^{+}_{B_T} &= \Delta B_T(+1\,\sigma_{I_{B_T}}) &= -2.5\log(2 - 10^{0.4\sigma^{-}_{B_T}}) \\ \sigma^{+}_{V_T} &= \Delta V_T(+1\,\sigma_{I_{V_T}}) &= -2.5\log(2 - 10^{0.4\sigma^{-}_{V_T}}) \end{aligned} \qquad [1.3.11]$$

As for B_T and V_T, the standard error interval of $B_T - V_T$ is not centred on the tabulated $B_T - V_T$ value, and one of the limits (or even both limits) could be undefined for a few stars. As described in Volume 4, Field T38 is derived from the larger of the two standard errors of $B_T - V_T$ (on the red and on the blue side, respectively), corresponding to $\pm 1\sigma_{I_{B_T}}$ and $\mp 1\sigma_{I_{V_T}}$. The individual uncertainties corresponding to $n\,\sigma_I$ are given approximately by:

$$\Delta(B_T - V_T)_{n\sigma_I} = 2.5\sqrt{[\log(1 + n - n\,10^{0.4\sigma^{-}_{B_T}})]^2 + [\log(1 - n + n\,10^{0.4\sigma^{-}_{V_T}})]^2} \qquad [1.3.12]$$

where n is negative on the blue side and positive on the red side; $\sigma^{-}_{B_T}$ and $\sigma^{-}_{V_T}$ are the uncertainties of B_T and V_T towards brighter magnitudes, as given in Fields T33 and T35 respectively.

The standard error of $(B - V)_J$ in Field T38 has been derived from Equations 1.3.12 and 1.3.22. The standard error of $(B - V)_T$ for a given Tycho star may be derived from the value in Field T38 by means of Equation 1.3.22, more simply than from Equation 1.3.12. Thus:

$$\sigma_{(B-V)_T} = \sigma_{(B-V)_J}/G \simeq \sigma_{(B-V)_J}/0.85 \qquad [1.3.13]$$

where G is given in Section 1.3 Appendix 4, Table 1.3.4.

Tycho Epoch Photometry Annex: Individual photometric observations in the B_T and V_T channels are provided in the Tycho Epoch Photometry Annex for a selection of the Tycho Catalogue entries. For each selected entry, a header record and a series of individual transit records are given. The header record contains summary photometric data, and also indicates the number of transit records following.

Two Tycho Epoch Photometry Annexes are published, differing in the number of catalogue entries for which transit records are included. Annex A, the smaller one, is part of the CD-ROM set in Volume 17 of the printed Hipparcos Catalogue. It contains transit data for 34 446 entries. The following groups of stars were selected (see Section 2.6 for details): (a) known or suspected variable stars and double stars; (b) a subset of the Tycho photometric standard stars. This selection was defined such as to include the most interesting subset of Tycho epoch photometry, while at the same time fitting onto a single CD-ROM.

Annex B, containing transit records for 481 553 catalogue entries, is archived at the CDS (Strasbourg). The selection includes all entries of Annex A, all stars brighter than $V_T = 10.25$ mag, and several small groups of stars of special interest. For details see Section 2.6.

The statistical significance of individual Tycho transits may be illustrated as follows. At $V_T = 9$ mag the mean photometric signal-to-noise ratio of a single slit group transit is of the order of 7. The censoring of transits is still fairly mild at this magnitude, but begins to become important at only slightly fainter magnitudes: the bias of a formal median magnitude is about 0.04 mag at $V_T = 9$ mag, increasing to about 0.20 and 0.80 mag at $V_T = 10$ and 11 mag.

Section 1.3 Appendix 1: Statistical Indicators

Different statistical indicators have been used to characterise the photometric stability or variability of stars in the Hipparcos and Tycho Catalogues, and the following provides a background to the choices made:

Quantiles: Let $x(p)$ denote the value of a random variable from a distribution, whose probability is p. Now consider N discrete (photometric) observations y_i, $i = 1...N$, ordered so that $y_i > y_{i-1}$. The observations y_i are mapped onto the distribution of $x(p)$ by setting $p = i/(N + 1)$, so that $x(p) = y_i$ for $i = 1...N$.

The complete distribution of $x(p)$ in [0,1] is then defined by the conventions $x(1/(N + 1)) = y_1$ and $x(N/(N + 1)) = y_N$. To this were added two artificial observations: $x(0) = x(1/(N + 1))$ and $x(1) = x(N/(N + 1))$, which avoids problems with estimates for low numbers of observations. The values of $x(p)$ at intermediate values of p are obtained by linear interpolation between adjacent points. $x(p)$ denotes the p-th quantile of the distribution. As explained below, different quantiles have been used as variability indicators in the case of the Hipparcos and Tycho Catalogues.

Error on the median: For the Hipparcos Catalogue entries, the median magnitude, m, is determined as $x(0.5)$. The standard error of $x(0.5)$ is given by:

$$\sigma_m = \frac{1}{2 f(z_{0.5}) \sqrt{N}} \qquad [1.3.14]$$

where $f(x)$ is the probability density function. For observations with identical variance σ^2 this reduces to:

$$\sigma_m = \sqrt{\frac{\pi}{2}} \frac{\sigma}{\sqrt{N}} \qquad [1.3.15]$$

representing a normal distribution of standard deviation σ. In the case of a variable star, the median may be very well defined despite large magnitude excursions in the observations. This is reflected in the expression for σ_m since the function $f(z_{0.5})$ represents the derivative of the cumulative probability function at the median. The expression for σ_m therefore conveys a local property of the observation distribution in the vicinity of the median, and remains largely insensitive to the wings, as does the median itself.

An evaluation of $f(z_{0.5})$, based on the difference of the empirical distribution function at the quantiles 0.35 and 0.65, provides a good compromise between the accuracy (being not far from the true slope) and the precision (since it includes, in general, a large number of data points). The resulting standard error on the median is then computed from:

$$\sigma_m = \frac{1}{\sqrt{N}} \frac{x(0.65) - x(0.35)}{0.615} \qquad [1.3.16]$$

where the coefficient 0.615 (or, more rigorously, 0.61488) is chosen such that the expectation of σ_m gives the factor $\sqrt{\frac{\pi}{2}}$ for a Gaussian distribution.

Scatter: the distribution of observations is ideally characterised by a small number of well-chosen parameters, less numerous than the observations themselves, but more than merely the location and its standard error. The scatter should provide information on the real scatter due to the noise, without being too much influenced by the variability, i.e. by the extended wings of the distribution.

The scatter of the observations has also been computed from specific percentiles of the distribution, while avoiding redundancy with the other characterisations of the distribution. A good compromise was to take the nearly half 2σ-width:

$$s = \frac{x(0.85) - x(0.15)}{2} \qquad [1.3.17]$$

whose expectation is 1.035σ for a Gaussian distribution. For constant stars, s gives an indication of the standard error of the individual observations, while a comparison with the maximum and minimum (defined in terms of the 5th and 95th percentiles of the distribution) can be taken as indicative of possible variability, since (min−max)/3.289 should be close to the sigma of an individual observation for a constant star.

In all calculations of medians, errors on medians and scatter values, it was assumed that all observations used had identical variances. This is not really true, and detailed interpretations of errors on medians, scatter values and other percentiles based data should be avoided. However, the median values are not expected to be seriously affected by different weights, and the expression used for calculating the errors on the median values still holds.

Section 1.3 Appendix 2: Variability Indicators

Proper investigation of variability of Hipparcos stars required careful assessment of the estimated errors on the Hipparcos epoch photometry. These error estimates were derived from a small number (between 5 and 10) of individual observations, each taking between 0.1 and 2 seconds. By calculating the variance of the mean from so few data points, a well-known bias is introduced, described by a Student's t distribution. These biases were empirically corrected by comparing the observed distributions of residuals for all standard stars with the expected distributions, as a function of magnitude and estimated error. Smooth corrections were determined and applied to the error estimates to bring them into agreement with the observed distributions. The resulting unit weight variance of the photometric data of a standard star is very close to 1.

Using the distribution of unit weight residuals, a χ^2 test was performed, comparing the observed distribution with a standard distribution based on about 20 000 apparently non-variable stars. This comparison distribution was close to Gaussian with unit variance, and independent of magnitude and colour. In the χ^2 test the residuals were binned according to the number of observations available and compared with the comparison distribution binned in the same way. Figure 1.3.2 shows the distribution of χ^2 values for all stars with at least 40 observations. In the following the 'χ^2 probability' refers to the formal probability of the star being constant, as based on the χ^2 test performed on the distribution of its unit weight residuals. Peculiarities recognised in the photometric data are summarised in Field H52 as follows:

Case 'C': All probably constant stars with the χ^2 probability larger than 0.5. In this context, constant means that the maximum undetectable amplitude is smaller than a magnitude-dependent threshold.

Case 'D': The distribution of unit weight residuals could also be affected by duplicity and colour errors (if the $(V-I)_{\rm C}$ index used in the reductions was erroneous). Duplicity could be recognised from two statistics: a comparison between the median ac and dc magnitudes, and a comparison between the estimated errors on the median ac and dc magnitudes (see Figure 1.3.3). Both indicators used the fact that for a double star the modulation amplitude is disturbed, and often indicates the presence of a fainter image than would be implied from the mean intensity. As explained in Section 1.3.1, the ac magnitude based statistic cannot be used for stars with the component flag set. These stars are also recognised as double in the double star processing, and are indicated as 'D' in Field H52.

Case 'M': Only stars with a χ^2 probability of less than 10^{-4} were considered in this category. The intrinsic amplitude of variability can only be estimated under certain assumptions—the assumption that the underlying signal is sinusoidal is reasonable for most small-amplitude pulsating and rotational modulation variables. Furthermore, it is assumed that the observed unit weight variance (U) is the sum of the variances caused by the measurement errors (= 1.0) and the weighted intrinsic variations, $U = I + 1.0$. If the mean squared weight of an observation is given by W, then the dispersion of the intrinsic variations is given by $A = \sqrt{I/W}$. For a sinusoidal signal $a\sin(\phi)$ a random sampling would produce a dispersion $A = a/\sqrt{2}$. The peak-to-peak amplitude of the underlying signal is then given by $A \times 2\sqrt{2} = 2a$. When below 0.03 mag, the variable is considered to be a 'micro-variable'. The underlying amplitude was considered insignificant when the value for (U) was less than 1.1. The coarse variability estimator (Field H6) was also derived from this amplitude estimate, dividing the intrinsic variability into three groups according to variability amplitude: '1' : less than 0.06 mag; '2' : between 0.06 and 0.6 mag; and '3' : more than 0.6 mag.

Case 'P' and case 'U': Stars which appeared to be variable were subjected to various period-searching algorithms, as well as compared with data available in the literature.

Case 'R': The epoch photometry for a star calibrated using an erroneous $(V-I)_C$ colour index shows up through a gradient with time in the data, and a systematic offset between the ac and dc magnitudes. Certain cases were flagged as described in Field H52. However, neither the epoch photometry, the summary photometry (Fields H44–46 and H49–50), or the epoch photometry header records were modified—any erroneous secular trends remain in the epoch photometry.

There is a certain amount of overlap between the various categories defined above. In Field H52 of the main catalogue this was dealt with through a strict setting of precedences (the resulting numbers of entries within each category are also given under Field H52). Every star passed through the following set of checks, in the given order, until it fulfilled one:

'R' : stars with confirmed $(V-I)_C$ error;
'P' : stars in variability annex Section 1 (periodic);
'U' : stars in variability annex Section 2 (unsolved);
'D' : stars with increased noise level on ac photometry;
'␣' : insufficient data for χ^2 statistics;
'C' : stars with probability > 0.5 of being constant;
'␣' : probability of being constant between 0.5 and 10^{-4};
'D' : remaining double stars;
'␣' : insignificant amplitude of variations;
'M' : micro-variables with amplitude below 0.03 mag;
'U' : remaining unsolved variables, not included in variability annex Section 2.

Since the Hipparcos photometry is photon noise limited, the detection threshold for variability (or for assessing constancy) is strongly magnitude dependent. Caution must therefore be exercised in considering whether stars flagged 'C' in Field H52 may be used as photometric standard stars. Stars flagged 'C' fainter than $Hp = 10$ mag, for example, will include most BY Dra, α Can Ven, β Cephei, and some δ Scuti stars. The amount of undetected variability ranges from a few millimagnitudes for the brighter stars, to several tenths of a magnitude at the fainter end.

The minimum peak-to-peak amplitude for the detection of confirmed variability is given in Table 1.3.3, which corresponds to the upper curve given in Figure 2.1.1 (under Field H52). The threshold for stars to be undetectable as variable is a factor of typically 0.88 of the quoted values, corresponding to the lower curve in Figure 2.1.1. The intermediate region corresponds to entries identified as suspected variables. Depending on the application, photometric standard stars may be selected according to any given maximum acceptable scatter. For catalogue entries with a number of photometric observations, N, differing from the mean value of about 110 (the actual number being given in Field H47) the corresponding threshold, T_N, scales approximately as:

$$T_N = T_{110}\sqrt{110/N} \qquad [1.3.18]$$

where T_{110} is the threshold corresponding to the mean number of photometric observations.

Table 1.3.3. The minimum peak-to-peak amplitude for stars to be confirmed as variables. Stars having detected variability at these levels have a probability of being constant of less than 0.001.

Hp	T_{110}	Hp	T_{110}	Hp	T_{110}
4.5	0.010	7.5	0.022	10.5	0.063
5.0	0.011	8.0	0.026	11.0	0.076
5.5	0.012	8.5	0.031	11.5	0.098
6.0	0.013	9.0	0.037	12.0	0.124
6.5	0.015	9.5	0.044	12.5	0.18
7.0	0.018	10.0	0.052	13.0	0.36

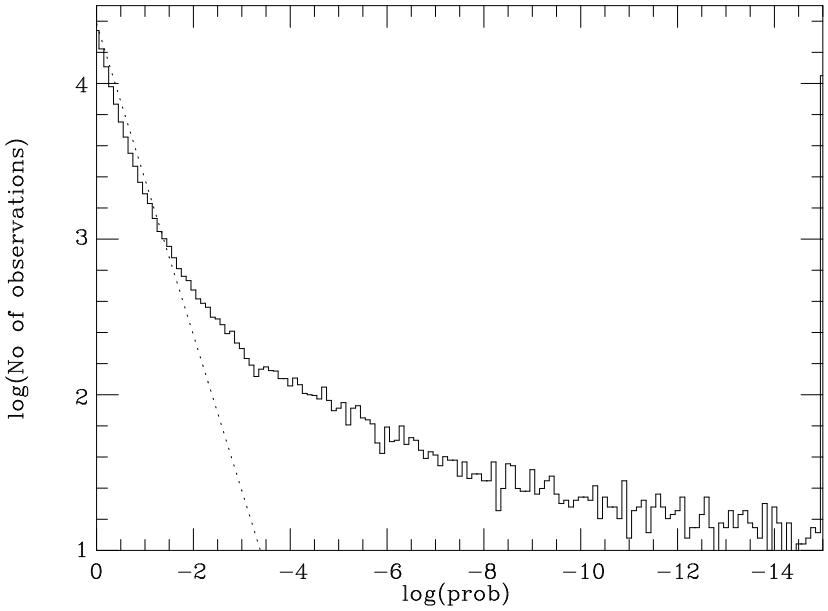

Figure 1.3.2. *The observed distribution of χ^2 values (full line) compared with the distribution for all stars being constant (dotted line).*

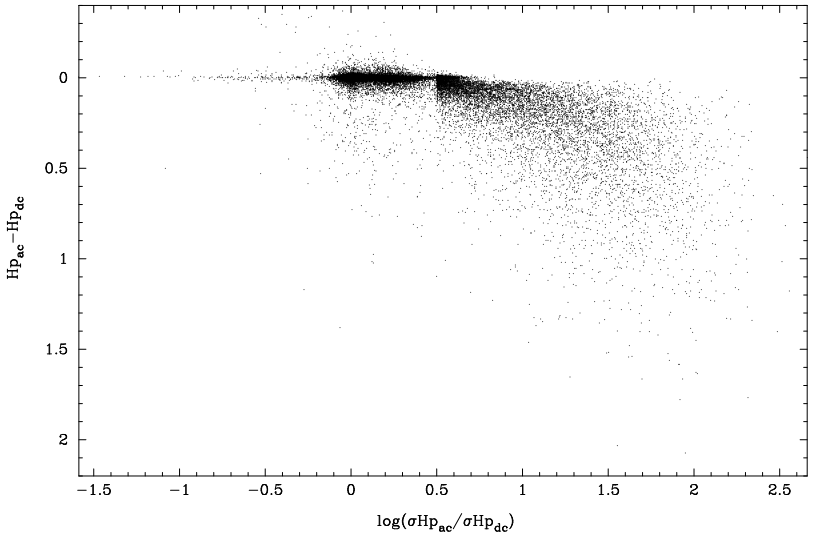

Figure 1.3.3. *The distribution of two statistical indicators of the Hipparcos Hp photometry. The noise ratio between the ac and the dc components increases for double stars, and the magnitude difference between the ac and dc components increases for double stars and extended objects. Variable stars can sometimes be found having smaller dispersion in the dc than in the ac component. For the central part of the diagram only a small selection of stars is displayed, in other parts all stars are shown.*

Section 1.3 Appendix 3: Period Optimisation and Amplitude Estimation

The periods detected with either the analysis of variance or the discrete Fourier analysis were hardly ever the optimal periods. The reason for this is that both methods assume certain characteristics of the data which in most cases are not fulfilled. This situation is made worse by the poor window functions characteristic of the Hipparcos data. Therefore, a simple procedure for fine-tuning the periods was developed that made use of the features of a given light curve. The following description applies strictly to the method used at the Royal Greenwich Observatory, whereas the method used at Geneva Observatory used different principles (see Volume 3 for details).

The first step was the fit of a spline function through the data, in such a way that the spline function was continuous in zero-, first- and second-order derivatives when going from phase 1 back to phase 0: the resulting fitted curve can be used as a periodic signal. The number of nodes and the positions of the nodes depend on the type of light curve and the total signal amplitude with respect to the noise on the data. In the case of some Algol-type variables a linear rather than a cubic spline was used.

If $f(\phi)$ is the function describing the light curve, and p is the period used to fold the signal, then the period correction can be obtained from a least-squares solution of the following observation equations:

$$O_i - f(\phi_i) = -\frac{t_i - t_0}{p}\frac{\Delta p}{p}\left(\frac{\partial f(\phi)}{\partial \phi}\right)_{\phi=\phi_i} \qquad [1.3.19]$$

where O_i represents observation i for which, when folded with period p the phase is given by $\phi_i = ((t_i - t_0)/p \bmod 1)$. The time of measurement (in barycentric Julian days) is give by t_i, while t_0 is an arbitrary zero-point roughly halfway through the total stretch of data. The new period is then $p' = p + \Delta p$.

The solution of this equation was iterated a few times with the solution for the curve fit $f(\phi)$, until period corrections became negligible. Solving the period through such an iteration had the advantage of optimising the period, while effectively putting most weight on those measurements that contain most information on the period: the measurements on the steepest parts of a light curve. The final solution provided an accuracy estimate for the period which, in most cases, appeared to be slightly on the optimistic side, and tends to depend to some extent on the actual curve fit $f(\phi)$. For automated processing, however, it was a practical solution, as it provided a measurement of the phases and magnitudes at minimum and maximum luminosity.

The amplitudes were derived from the maximum and minimum values of the fitted light curves. If the covariance matrix of the least-squares solution for $f(\phi)$ is given by A^{-1}, then the precision of the estimated value at a given phase ϕ can be derived from $\sigma f = s\sqrt{(f A^{-1} f^T)}$, where s is the standard deviation of the least-squares solution. The error on the amplitude was then calculated from the errors of the minimum and maximum magnitudes.

Section 1.3 Appendix 4: Photometric Transformations

The Hipparcos Hp photometry and the Tycho B_T and V_T photometry are the most substantial uniformly accurate collection of photometric data ever realised. At the time of the catalogue publication, the number of stars accurately measured by Hipparcos has already exceeded the number of stars measured in the major photometric system, Johnson UBV, during the past 45 years (some 108 000 stars).

The Hp magnitudes define a photometric reference system over the whole sky with an unprecedented accuracy, free from systematic errors as a function of right ascension or declination, and free from magnitude scale errors at the millimagnitude level. The Tycho two-colour system should also be considered as a new independent system, also free from systematic errors as a function of right ascension or declination, with only small departures from linearity at the bright and faint ends (at the faint end the possible systematic errors may be comparable to the quoted standard error). To avoid degrading these accuracies through approximate transformations it is recommended to use the magnitudes Hp, B_T and V_T directly, and to calibrate them in terms of astrophysical quantities.

Transformations used for the Tycho Catalogue

Using values of Johnson V_J and $(B-V)_J$ for 8000 standard stars with good Tycho (B_T, V_T) photometry, the following approximate linear transformations were derived between the two systems over the range $-0.2 < (B-V)_T < 1.8$:

$$\begin{aligned} V_J &= V_T - 0.090\,(B-V)_T \\ (B-V)_J &= 0.850\,(B-V)_T \end{aligned} \qquad [1.3.20]$$

giving errors generally below 0.015 mag in V_J and below 0.05 mag in $(B-V)_J$. The transformations apply to unreddened stars and ignore variations due to luminosity class. They should not be applied to M-type stars, even for $(B-V)_T < 1.8$ mag.

A more accurate transformation is obtained by linear interpolation of the values given in Table 1.3.4, where the factor G provides the slope of the local $(B-V)_J$ versus $(B-V)_T$ relation, and the values tabulated at the ends of the given interval are used for extrapolation. These relations have been used for the $(B-V)_J$ colour index given in the Tycho Catalogue. The formal errors on V_J and $(B-V)_J$ are well approximated by:

$$\sigma_{V_J} = \sqrt{1.09\,\sigma^2_{V_T} + 0.09\,\sigma^2_{B_T}} \qquad [1.3.21]$$

and:

$$\sigma_{(B-V)_J} = G \times \sigma_{(B-V)_T} \simeq G \times \sqrt{\sigma^2_{V_T} + \sigma^2_{B_T}} \qquad [1.3.22]$$

These equations do not take account of reddening and luminosity class (see Figure 1.3.6). The square root approximation in Equation 1.3.22 is only satisfactory if the errors of B_T and V_T are less than about 0.1 mag. For the computation of $\sigma_{(B-V)_J}$ in Field T38 the more accurate expression in Equation 1.3.12 has been used.

Table 1.3.4. Transformation from the Tycho photometric system to Johnson. The points given can be used in a linear interpolation, with deviations less than 0.005 mag from a more accurate spline fit.

$(B-V)_T$	≤ -0.2	0.1	0.5	1.4	≥ 1.8	
$V_J - V_T + 0.090(B-V)_T$	0.014	0.000	−0.005	−0.005	−0.015	
$(B-V)_J - 0.85(B-V)_T$	−0.006	0.000	0.046	−0.008	−0.032	
G-factor	0.85	0.87	0.97	0.79	0.79	0.85

Transformations used for the Hipparcos Catalogue

By construction, the Hp, B_T, V_T system is linked and normalised to the Johnson system by the conditions:

$$\begin{aligned} Hp &\equiv 0 \qquad \text{for } V_J = 0 \text{ and } B - V = 0 \\ V_T &\equiv 0 \qquad \text{for } V_J = 0 \text{ and } B - V = 0 \\ B_T &\equiv 0 \qquad \text{for } B_J = 0 \text{ and } B - V = 0 \end{aligned} \qquad [1.3.23]$$

The Relationship between Hp and V_J

The photometric data have been calibrated in the true instrumental Hp system as defined at a particular reference epoch. The actual response curve of Hp was a function of time, and the reference system that was implemented represents the Hp response for a date that was anticipated to be close to the middle of the mission, 1 January 1992. It applies strictly to the dc magnitudes (see Section 2.5 for details). There are very small differences in the time-dependent response function for the ac magnitudes, which have not been fully calibrated.

The definition of $(Hp - V_J)$ computed *a priori* on the basis of the instrumental calibration carried out on ground (on the basis of the nominal Hp response and stellar spectrophotometry) had to be revised in orbit for very red stars. The redetermination of the Hp response, and of the relation $(Hp - V_J)$, was problematic for stars redder than $(V - I)_C \sim 3.0$ mag because all such objects are highly variable, and therefore required simultaneous observations from the satellite and from the ground in order to provide a meaningful calibration.

The relationship was established by observing a set of long-period variables, of C and M type, with a CCD chain equipped with the Cousins' I band and Johnson/Geneva V band, in order to obtain $(V - I)_C$ and, immediately before or after, to measure the same Mirae with a classical photometer, to provide the original V_J magnitude. In parallel, AAVSO observers were requested to monitor these stars. This made it possible to define the relation $(V_{CCD} - V_J)$ versus $(V - I)_C$ and, at the epochs of photoelectric observations, the relations $(V_{AAVSO} - V_{CCD})$ and $(V_{AAVSO} - V_J)$. Hp magnitudes were deduced from the non-linear relations $(V_{AAVSO} - Hp)$ versus V_{AAVSO} as observed during the mission.

The resulting $(Hp - V_J)$ versus $(V - I)_C$ is very well defined from classical photometry in the range $-0.4 < V - I < 3.0$ mag, with uncertainties of less than 0.01 mag. The red extension down to $V - I = 5.4$ mag was defined using Mirae, with an uncertainty of 0.03–0.05 mag. Between $V - I = 3.8 - 5.4$ mag, this relation is linear. The values down to $V - I = 9.0$ mag follow from a linear extrapolation: they are given in order to cover the whole range of $(V - I)_C$ colours in the Hipparcos Catalogue.

The relation given in Table 1.3.5 holds, in principle, for O, B, A, F, G < G5 stars with low reddening, and for G5 to M8 giants. The relation for G, K and M dwarfs is given in Table 1.3.6. The difference between both relations is rather small, i.e. less than 0.030 mag. Figure 1.3.4 shows the transformations in graphical form.

Restrictions on the validity of these transformation equations for peculiar stars are the same as those described under the transformations for $(B - V)$ versus $(B_T - V_T)$.

Table 1.3.5. $(Hp - V_J)$ versus $(V - I)_C$ for spectral types O to G5 luminosity class II to V, and red giants of types G5III to M8III.

$V-I$	$Hp-V_J$	$V-I$	$Hp-V_J$	$V-I$	$Hp-V_J$	$V-I$	$Hp-V_J$
−0.50	−0.182	0.40	0.082	1.30	0.153	2.90	−0.065
−0.45	−0.164	0.45	0.089	1.35	0.147	3.00	−0.090
−0.40	−0.145	0.50	0.097	1.40	0.140	3.20	−0.155
−0.35	−0.126	0.55	0.106	1.45	0.135	3.40	−0.235
−0.30	−0.107	0.60	0.115	1.50	0.128	3.60	−0.325
−0.25	−0.088	0.65	0.125	1.60	0.116	3.80	−0.425
−0.20	−0.070	0.70	0.133	1.70	0.106	4.00	−0.535
−0.15	−0.053	0.75	0.141	1.80	0.096	4.20	−0.65
−0.10	−0.035	0.80	0.147	1.90	0.090	4.40	−0.76
−0.05	−0.018	0.85	0.154	2.00	0.082	4.60	−0.87
0.00	0.002	0.90	0.159	2.10	0.072	4.80	−0.98
0.05	0.018	0.95	0.164	2.20	0.060	5.00	−1.10
0.10	0.036	1.00	0.167	2.30	0.048	5.50	−1.38
0.15	0.050	1.05	0.168	2.40	0.032	6.00	−1.66
0.20	0.061	1.10	0.168	2.50	0.018	6.50	−1.94
0.25	0.068	1.15	0.165	2.60	0.001	7.00	−2.22
0.30	0.072	1.20	0.162	2.70	−0.018	8.00	−2.78
0.35	0.076	1.25	0.157	2.80	−0.040	9.00	−3.34

Table 1.3.6. $(Hp - V_J)$ versus $(V - I)_C$ for G, K, M dwarfs with $(V - I)_C > 0.70$ mag.

$V-I$	$Hp-V_J$	$V-I$	$Hp-V_J$	$V-I$	$Hp-V_J$	$V-I$	$Hp-V_J$
0.70	0.133	1.10	0.138	1.50	0.108	2.20	0.051
0.75	0.137	1.15	0.133	1.55	0.105	2.30	0.041
0.80	0.140	1.20	0.129	1.60	0.102	2.40	0.034
0.85	0.142	1.25	0.125	1.70	0.093	2.50	0.022
0.90	0.144	1.30	0.122	1.80	0.085	2.60	0.001
0.95	0.146	1.35	0.119	1.90	0.076	2.70	−0.023
1.00	0.145	1.40	0.115	2.00	0.066		
1.05	0.142	1.45	0.112	2.10	0.058		

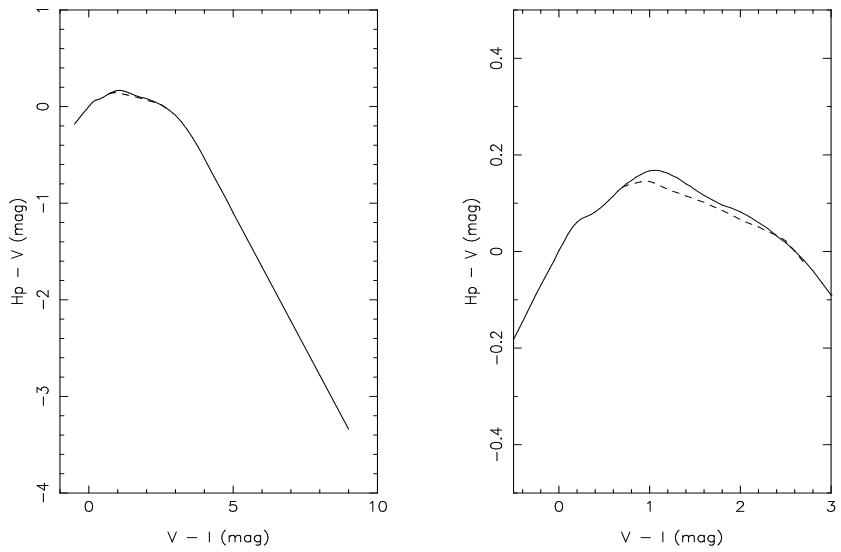

Figure 1.3.4. *The relation* $(Hp - V_J)$ *versus* $(V-I)_C$ *for different ranges of* $(V-I)_C$. *Solid lines: for spectral types O to G5 luminosity class II to V, and red giants of types G5III to M8III (from Table 1.3.5). Dashed lines: for G, K, M dwarfs with* $(V-I)_C$ *>0.70 mag (from Table 1.3.6).*

$(B-V)$ derived from $(B_T - V_T)$

Since the Tycho passbands, B_T and V_T (and in particular B_T), are different from the corresponding Johnson B, spectral features such as Balmer lines or molecular lines for late-type stars introduce differential effects, as do interstellar or circumstellar reddening. As a consequence, different relations are applicable to various spectral ranges, and must be separately applied in order to minimise the residuals arising from the transformation. The most sensitive spectral types from this point of view are the A-type stars, late-M, and Carbon stars. The following relations were used in the determination of the $B-V$ index based on $B_T - V_T$ (see Field H39) as a function of spectral type. Figure 1.3.5 illustrates the luminosity dependence and Figure 1.3.6 illustrates the effects of reddening for cases (a–c).

(a) for dwarfs (luminosity class V):

$B_T - V_T < 0.345$:

$$(B-V) = (B_T - V_T) + 0.021 - 0.130z - 0.08z^2 + 0.430z^3$$
$$z = B_T - V_T + 0.15 \qquad [1.3.24]$$

$0.345 < B_T - V_T < 0.50$:

$$(B-V) = (B_T - V_T) - 0.041 - 0.262z - 0.30z^2 + 1.030z^3$$
$$z = B_T - V_T - 0.60 \qquad [1.3.25]$$

$0.50 < B_T - V_T$:

$$(B-V) = (B_T - V_T) - 0.115 - 0.229z + 0.043z^3$$
$$z = B_T - V_T - 0.90 \qquad [1.3.26]$$

(b) for giants (luminosity class III with low reddening) with $B_T - V_T < 1.7$ mag:

$B_T - V_T < 0.65$:

$$(B-V) = (B_T - V_T) - 0.010 - 0.060z - 0.14z^3$$
$$z = B_T - V_T - 0.22 \qquad [1.3.27]$$

$0.65 < B_T - V_T < 1.10$:

$$(B-V) = (B_T - V_T) - 0.113 - 0.258z + 0.40z^3$$
$$z = B_T - V_T - 0.95 \qquad [1.3.28]$$

$1.10 < B_T - V_T$:

$$(B-V) = (B_T - V_T) - 0.173 - 0.220z + 0.01z^3$$
$$z = B_T - V_T - 1.20 \qquad [1.3.29]$$

(c) for late K giants, and luminous G and K stars (luminosity class I to II) with $B_T - V_T > 1.7$ mag:

$1.0 < B_T - V_T < 2.2$:

$$(B-V) = (B_T - V_T) - 0.173 - 0.220z + 0.01z^2$$
$$z = B_T - V_T - 1.20 \qquad [1.3.30]$$

(d) for Carbon stars, often surrounded by dust and showing extreme red colours:

$$(B-V) = +0.19 + 0.73\,(B_T - V_T) \qquad [1.3.31]$$

(e) for M giants, affected by the presence of TiO bands:

$$(B-V) = +0.046 + 0.824\,(B_T - V_T) \qquad [1.3.32]$$

When no luminosity classification was available, the relation defined for luminosity class III giants was used.

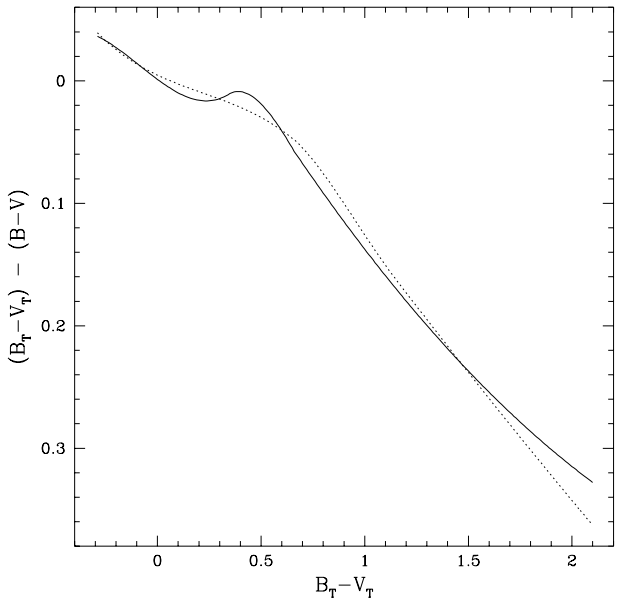

Figure 1.3.5. *The luminosity dependence of* $(B-V)$ *on* (B_T-V_T)*. The solid line corresponds to luminosity class V stars, while the dotted line corresponds to class III giants. The gravity effect, observable primarily through different absorption from the Balmer lines in* B_T *and* V_T*, reaches a maximum at around* B_T-V_T *~0.4 mag.*

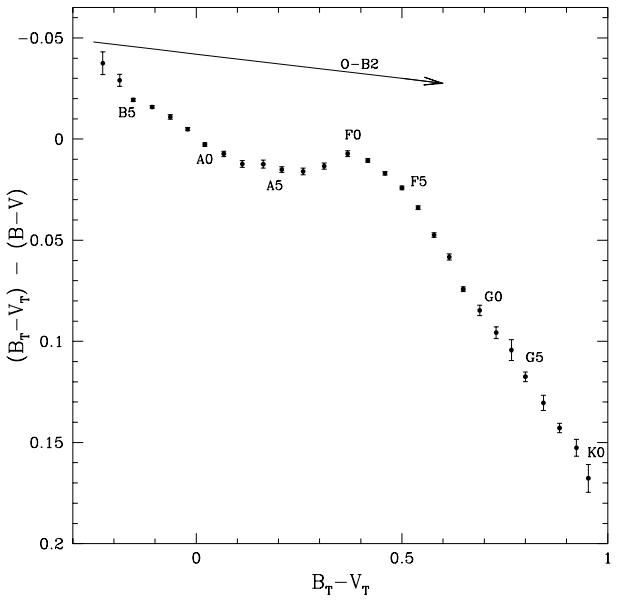

Figure 1.3.6. *The effect of reddening on the relationship between* $(B-V)$ *and* (B_T-V_T)*. The circles indicate the observed relationship for luminosity class V stars with accurate photoelectric photometry. The solid line shows the mean reddening direction for O–B2 stars (independent of luminosity class). Reddening for later-type stars moves the corresponding points parallel to this line.*

V_J derived from V_T

(a) for early-type stars and red stars up to and including K-type, the following relation is applicable to both dwarfs and giants:

$$V_J = V_T + 0.0036 - 0.1284(B_T - V_T) + 0.0442(B_T - V_T)^2 - 0.015(B_T - V_T)^3 \quad [1.3.33]$$

(b) for Carbon stars (R, N, C):

$$V_J = V_T + 0.007 - 0.024(B_T - V_T) - 0.023(B_T - V_T)^2 \quad [1.3.34]$$

(c) for M giants, the differential absorption by TiO, depending on the stellar temperature, metallicity, and gravity, means that the index $V_T - V_J$ becomes unrelated to $B_T - V_T$, since $(B_T - V_T)$ reaches a saturation value around 1.95, and then decreases again to about 1.45 for M5 stars. An indirect approach, allowing the degeneracy for M stars to be circumvented, consists of first evaluating the $V - I$ index from the $(Hp - V_T)$ versus $(B_T - V_T)$ relation, then applying a $(V_T - V_J)$ correction as a function of $(V - I)$ (see Figure 1.3.7). This results in the following relations:

$$\begin{aligned} V - I &= 3.55 - 2.44(dH + 0.60) - 0.60(dH + 0.60)^2 \qquad dH < 0.25 \\ V - I &= 2.02 - 6.00(dH + 0.12) - 11.0(dH + 0.12)^2 \qquad dH > 0.25 \end{aligned} \quad [1.3.35]$$

where $dH = (Hp - V_T) - 0.41(B_T - V_T - 1.9)^2$. V_J is then given by:

$$V_J = V_T - 0.20 - 0.03(V - I - 2.15) - 0.011(V - I - 2.15)^2 \quad [1.3.36]$$

(d) for M dwarfs, no relation between V_J and V_T has been defined, since all are too faint in B_T to provide a $B_T - V_T$ index precise enough to determine V_J from V_T and $B_T - V_T$.

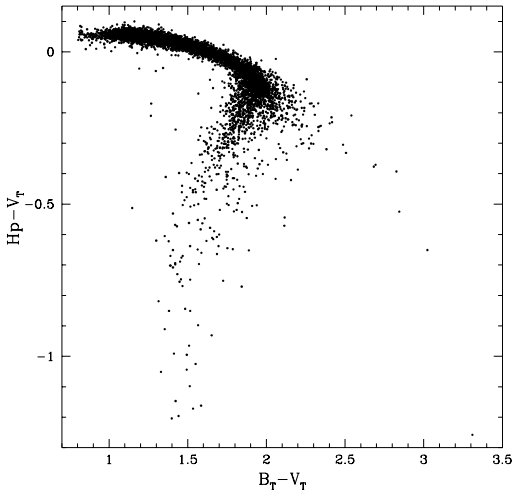

Figure 1.3.7. *The observed $(Hp - V_T)$ versus $(B_T - V_T)$ diagram for red giants. The G and K giants, and some Carbon stars, occupy the well-populated upper part of the diagram extending roughly horizontally up to $B_T - V_T$ ~2 mag (with reddened objects continuing in a descending arc towards the bottom right of the figure). The O-rich M stars form the descending sequence, with a vertical displacement from the region populated by the G–K giants being a direct measurement of the differential absorption on Hp and V_T, and directly related to the $V - I$ index (the decrease of $(B_T - V_T)$ with decreasing $Hp - V_T$ is due to an excess of TiO absorption on V_T relative to B_T).*

Section 1.3 Appendix 5: Determination of the $V - I$ Colour Index

The flag in Field H42 indicates the method adopted to estimate $(V - I)_C$. Twenty different methods were defined and applied in order to produce $(V-I)_C$ for all Hipparcos stars, and in the description below they are ranked according to their hierarchy of application. The reliability of the methods used may be inferred through the standard error on $(V - I)_C$ given in Field H41.

The $(V - I)_C$ colour index was determined to be the most appropriate to correct for chromatic residuals in the reduction of the astrometric data and, more importantly, for the photometric reductions, where the magnitudes were affected by colour-dependent transmission losses. In the context of Hipparcos, the $(V - I)_C$ index provided a way of monitoring and correcting for the chromatic evolution of the optics, applicable to stars of all colours, including the reddest long-period variables.

For a small fraction of the stars, the genuine Cousins' $(V - I)_C$ was available. Only when $(V - I)_C$ was derived from similar photometric systems are the photometric properties of this index, such as a temperature estimator with little dependence on reddening or metallicity, preserved.

When derived from other colour indices, the abundance and reddening dependencies affecting these indices are propagated into the resulting pseudo $(V - I)_C$ index. In stars with VRI photometry, an approximate $(V - I)_C$ was transformed from ground-based multi-colour photometric data, or from star mapper data with or without spectral-type information, or from a combination of an approximate $(B - V)$ and of the spectral type. Multi-colour photometric data necessary to produce $(V - I)_C$ were extracted from the General Catalogue of Photometric Data (GCPD), compiled at the Lausanne Institute of Astronomy (B. Hauck *et al.*, 1990, *Astronomy & Astrophysics Supplement*, 85, 989–998), and updated at mid-mission and at the end of the data reduction process.

For late-type stars, distinct relations were used for main-sequence and for giants, assuming a solar metallicity. The separation between dwarfs and giants was made according to an 'absolute magnitude estimator' (see method I). Ambiguous cases were treated individually using all external information, including some of the Hipparcos absolute magnitudes.

V, R, I Photometry (A–G)

Field H42 = A: $(V - I)_C$ measured directly in the Cousins' system. Only 2989 Hipparcos programme stars had genuine Cousins' $(V - I)_C$ colour index. They are mainly nearby parallax stars and metal poor stars. When several sources of data were available the weighted mean, and the precision on the mean $(V - I)_C$, were computed.

Field H42 = B: If only $(V - R)_C$ was available, the following transformations were applied:

$(V - R)_C$	$(V - I)_C$
< 0.0	$2.50\,(V - R)_C$
$[0.0, 0.6]$	$2.04\,(V - R)_C - 0.205\,(V - R)_C^2$
$[0.6, 1.0]$	$1.60\,(V - R)_C + 0.61\,(V - R)_C^2 - 0.034$
> 1.0	$2.70\,(V - R)_C - 0.52$

Field H42 = C: When stars were measured in the Johnson V, R, I system, and only $(V-I)_J$ was available, the following relations were used—when V_J and I_J were published separately, a zero point shift was needed to convert the raw magnitude difference into the classical $(V-I)_J$:

$(V-I)_J$	$(V-I)_C$
< 0.0	$0.713\,(V-I)_J$
$[0.0, 2.0]$	$0.778\,(V-I)_J$
$]2.0, 3.0]$	$0.835\,(V-I)_J - 0.13$

Field H42 = D: When stars were measured in the Johnson V, R, I system, and only $(V-R)_J$ was available, it was transformed into $(V-R)_C$ by the following relations (and then into $(V-I)_C$ by the relations given for method B):

$(V-R)_J$	$(V-R)_C$
< 1.0	$0.73\,(V-R)_J - 0.03$
> 1.0	$0.62\,(V-R)_J - 0.03$

Field H42 = E: When stars were measured in the Kron-Eggen V, R, I system, and $(V-I)_K$ was known, the transformation used was:

$(V-I)_K$	$(V-I)_C$
< 0.5	$0.936\,(V-I)_K + 0.27$
> 0.5	$1.000\,(V-I)_K + 0.24$

Field H42 = F: When stars were measured in the Kron-Eggen V, R, I system, and only $(R-I)_K$ was known, it was transformed into $(R-I)_C$ as follows:

$(R-I)_K$	$(R-I)_C$
$[0.29, 0.65]$	$1.049\,(R-I)_K + 0.092$
$]0.65, 1.15]$	$1.205\,(R-I)_K - 0.008$

$(R-I)_C$ was then transformed into $(V-I)_C$ as follows:

$(R-I)_C$	$(V-I)_C$
< 0.10	$1.69\,(R-I)_C$
$[0.10, 0.50]$	$2.26\,(R-I)_C - 0.05$
$]0.50, 0.75]$	$1.84\,(R-I)_C + 0.17$
> 0.75	$1.49\,(R-I)_C + 0.43$

Field H42 = G: When several V, R, I sources were available, a weighted mean was computed and the resulting $(V-I)_C$ index compiled using the appropriate combination of methods described above.

Multi–colour Photometry (H–K)

Field H42 = H: The $(B-V)_J$ colour from Johnson UBV system was transformed into $(V-I)_C$ according to the following transformations tabulated separately for early-type stars and red giants, and for late-type dwarfs. For stars with $(B-V)_J < 0.9$ mag, $(V-I)_C$ was interpolated in Table 1.3.7. Other categories derived from Table 1.3.7 are discussed under Field H42 = I, J, and K.

When stars had been observed in the Geneva, Strömgren and Walraven systems, colour indices of each system were first transformed into $(B-V)_J$, then transformed into $(V-I)_C$, as in the case of Johnson UBV data. Method H was used irrespective of the multi–colour system(s) used to produce $(V-I)_C$.

Table 1.3.7. $(V-I)_C$ versus $(B-V)_J$ for early-type stars and red giants

$(V-I)_C$	$(B-V)_J$	$(V-I)_C$	$(B-V)_J$	$(V-I)_C$	$(B-V)_J$	$(V-I)_C$	$(B-V)_J$
−0.379	−0.345	0.190	0.174	0.804	0.765	1.334	1.365
−0.299	−0.276	0.252	0.228	0.847	0.825	1.392	1.413
−0.231	−0.216	0.331	0.291	0.897	0.893	1.473	1.464
−0.168	−0.164	0.412	0.351	0.946	0.960	1.567	1.527
−0.105	−0.119	0.482	0.415	0.995	1.021	1.617	1.550
−0.050	−0.072	0.553	0.482	1.050	1.088	1.644	1.568
0.002	−0.020	0.617	0.543	1.107	1.143	1.724	1.583
0.040	0.021	0.667	0.597	1.155	1.196	1.831	1.604
0.072	0.062	0.722	0.659	1.211	1.253	1.882	1.615
0.124	0.110	0.770	0.717	1.271	1.311	2.021	1.635

Field H42 = I: Redder stars were separated into red giants, red dwarfs and long-period variables according to the value of the absolute magnitude estimator, M, defined as follows:

$$M = V_J + 5.0 \log_{10} (\text{proper motion}) + 1.505$$

where the proper motion is expressed in arcsec/yr. M larger than 5.2 indicates a late-type dwarf or a high-velocity giant. Marginal cases were treated star by star. For red giants with $(B-V)_J < 1.25$ mag, $(V-I)_C$ was derived from Table 1.3.7. Otherwise, for these late-type K and M dwarfs, $(V-I)_C$ was derived (Table 1.3.8) as follows:

Table 1.3.8. $(V-I)_C$ versus $(B-V)_J$ for late-type K and M dwarfs

$(V-I)_C$	$(B-V)_J$	$(V-I)_C$	$(B-V)_J$	$(V-I)_C$	$(B-V)_J$	$(V-I)_C$	$(B-V)_J$
0.631	0.550	1.042	0.999	1.567	1.348	2.725	1.650
0.670	0.601	1.103	1.050	1.645	1.390	2.874	1.700
0.707	0.648	1.175	1.100	1.785	1.445	3.008	1.750
0.747	0.699	1.244	1.149	1.905	1.472	3.144	1.800
0.788	0.749	1.333	1.199	2.054	1.498	3.478	1.900
0.840	0.800	1.386	1.228	2.255	1.524	3.630	1.955
0.893	0.850	1.410	1.250	2.440	1.550	4.100	2.114
0.941	0.898	1.494	1.300	2.544	1.575	4.328	2.198
0.997	0.949	1.535	1.326	2.601	1.600	4.630	2.300

Field H42 = J: Stars redder than $(B-V)_J = 1.25$ mag were treated according to their spectral type. For R, N, C type stars, the following linear relation was adopted:

$$(V-I)_C = 1.042\,(B-V)_J - 0.047$$

Reddened F, G, K < K5 stars, with $B-V > 1.55$ mag, follow the same relation. Otherwise their $(V-I)_C$ were interpolated in Table 1.3.7.

Field H42 = K: For giant stars later than K4, $(B-V)_J$ and $(V-I)_C$ become affected by TiO bands absorption. At a given $(B-V)_J$, the departure from the linear relation defining $(V-I)_C$ used for method J is a steep function of the spectral type, especially for the late-M sub-types. S and M types were not distinguished here. In this case, $\sigma_{(V-I)_C}$ is equal to $1.042\sigma_{(B-V)_J}$ added quadratically to σ_{type}, the observed scatter in $(V-I)_C$ for a given K or M sub-type.

Table 1.3.9. $(V-I)_C$ versus $(B-V)_J$ for giants later than K4

Type	$(V-I)_C$	σ_{type}	Type	$(V-I)_C$	σ_{type}
K5	$1.042\,(B-V)_J - 0.015$	0.09	M4	$1.042\,(B-V)_J + 0.978$	0.50
K5-9	$1.042\,(B-V)_J - 0.045$	0.14	M4.5	$1.042\,(B-V)_J + 1.329$	0.75
M0	$1.042\,(B-V)_J + 0.109$	0.15	M5	$1.042\,(B-V)_J + 1.679$	0.83
M0.5	$1.042\,(B-V)_J + 0.184$	0.16	M5.5	$1.042\,(B-V)_J + 2.040$	0.82
M1	$1.042\,(B-V)_J + 0.259$	0.17	M6	$1.042\,(B-V)_J + 2.399$	0.80
M1.5	$1.042\,(B-V)_J + 0.333$	0.18	M6.5	$1.042\,(B-V)_J + 2.754$	0.80
M2	$1.042\,(B-V)_J + 0.408$	0.21	M7	$1.042\,(B-V)_J + 3.109$	0.80
M2.5	$1.042\,(B-V)_J + 0.518$	0.22	M8.5	$1.042\,(B-V)_J + 3.459$	0.80
M3	$1.042\,(B-V)_J + 0.628$	0.30	M8	$1.042\,(B-V)_J + 3.820$	0.80
M3.5	$1.042\,(B-V)_J + 0.803$	0.37	M8+	$1.042\,(B-V)_J + 4.170$	0.80

$V-I$ from Hipparcos and Star Mapper Photometry (L–P)

At the beginning of the mission some 50 800 programme stars had no accurate ground-based photoelectric photometry, but were subsequently observed by the satellite's star mapper. The reduction of brighter star transits led to provisional B_T and V_T magnitudes. An updating of approximate $(B-V)_J$ given in the Hipparcos Input Catalogue was made at mid-mission using these provisional values, thus allowing an improvement in the final photometric and astrometric reductions to be made. Stars of types O to K4 had to be processed differently from the later type stars, the division being made according to the object's location in the provisional $(Hp-V_T)/(B_T-V_T)$ diagram.

At the very end of the data reduction phase the final Tycho photometric data then became available for about 113 000 stars. Most of the non-photoelectric $(V-I)_C$ could then be superseded by more accurate $(V-I)_C$ determined from (B_T-V_T) and partly from the relationship $(Hp-V_T)$ versus (B_T-V_T).

Except for M giants, (B_T-V_T) were first transformed into $(B-V)$ and then into $(V-I)_C$. Although carried out according to methods H, I, and J, these entries are all labelled as method L since they used colour indices from Tycho. M giants had their $(V-I)_C$ determined from an updated version of method O given under the description of the (B_T-V_T) to $(B-V)$ transformations in Section 1.3, Appendix 4. They are still flagged as method O.

As a result, methods M–P described below have an almost historical character, since they refer to stars, not reprocessed with the final Tycho photometric data; furthermore, since they make use of intermediate Hp and B_T-V_T which are no longer valid, the affected indices carry the subscript '*'.

Field H42 = L: The condition $(Hp-V_T)_*-0.786\,(B_T-V_T)_*+1.272<0$ selects stars without TiO absorption. Blue stars show a linear relation between $(B_T-V_T)_*$ and $(V-I)_C$. For $(B_T-V_T)_*<-0.05$ mag:

$$(V-I)_C = 1.192\,(B_T-V_T)_* + 0.058$$

For $-0.05<(B_T-V_T)_*<1.80$ mag, $(V-I)_C$ was obtained by interpolation in Table 1.3.10.

Table 1.3.10. $(V-I)_C$ versus $(B_T-V_T)_*$ for O to G stars, and K < K5 giants

$(V-I)_C$	$(B_T-V_T)_*$	$(V-I)_C$	$(B_T-V_T)_*$	$(V-I)_C$	$(B_T-V_T)_*$	$(V-I)_C$	$(B_T-V_T)_*$
−0.302	−0.326	0.136	0.152	0.597	0.557	0.977	1.151
−0.250	−0.258	0.177	0.193	0.630	0.591	1.006	1.200
−0.184	−0.202	0.217	0.225	0.658	0.642	1.040	1.250
−0.132	−0.165	0.248	0.252	0.690	0.684	1.075	1.300
−0.101	−0.135	0.284	0.282	0.719	0.726	1.112	1.350
−0.059	−0.096	0.337	0.317	0.754	0.773	1.155	1.400
−0.007	−0.047	0.398	0.357	0.790	0.829	1.210	1.467
0.024	0.014	0.441	0.392	0.832	0.892	1.262	1.536
0.053	0.052	0.476	0.429	0.866	0.957	1.330	1.611
0.069	0.085	0.529	0.480	0.908	1.026	1.403	1.679
0.103	0.118	0.569	0.520	0.939	1.084	1.492	1.756
						1.600	1.809

Field H42 = M: For stars with $(Hp-V_T)_*-0.786\,(B_T-V_T)_*+1.272>0$, the following relation was used for reddened G and K < K5 stars (assumed to be giants):

$$(V-I)_C = 1.156\,(B_T-V_T)_* - 0.532$$

Field H42 = N: For stars with $(Hp-V_T)_*-0.786\,(B_T-V_T)_*+1.272>0$, the following relations were used for K5 to M0.5 giants:

Type	$(V-I)_C$
K5	$1.156\,(B_T-V_T)_* - 0.500$
K5.5	$1.156\,(B_T-V_T)_* - 0.440$
M0	$1.156\,(B_T-V_T)_* - 0.376$
M0.5	$1.156\,(B_T-V_T)_* - 0.301$

Field H42 = O: For later M giants and for Carbon stars, iso-$(V-I)_C$ lines were defined in the $(Hp-V_T)_*/(B_T-V_T)_*$ diagram. For stars bluer than $(B_T-V_T)_*=2.8$ mag, $(V-I)_C$ was obtained for unreddened and reddened stars as follows:

(a) for $(Hp-V_T)_*-0.41\,[(B_T-V_T)_*-1.9]^2<0.05$:

$$(V-I)_C = -5.4\,\{(Hp-V_T)_*-0.41\,[(B_T-V_T)_*-1.9]^2\}+2.61$$

(b) for $(Hp-V_T)_*-0.41\,[(B_T-V_T)_*-1.9]^2>0.05$:

$$(V-I)_C = -7.0\,\{(Hp-V_T)_*-0.41\,[(B_T-V_T)_*-1.9]^2\}+2.68$$

Field H42 = P: Stars with $(B_T-V_T)_*>2.8$ mag are either Carbon stars or reddened G, K, or M supergiants. Their $(V-I)_C$ was estimated by the relation:

$$(V-I)_C = 0.890\,(B_T-V_T)\,* - 0.005$$

Long-Period Variables (Q)

Field H42 = Q: Long-period variables required a special treatment. Very few have been monitored over the whole light-curve cycle. In the photometric data base, the colour and the magnitude at maximum luminosity is normally given, rather than a mean colour index and magnitude, which are rarely defined. In order not to underestimate their mean colour index, the spectral type at maximum and minimum luminosity were searched for in the literature. This information was missing in the Hipparcos Input Catalogue, since complex spectral types were truncated.

A mean type was computed for each long-period variable; $(V-I)_C$ and $\sigma_{(V-I)_C}$ were deduced by linear interpolation in Table 1.3.11. Since the $E(V-I)_C$ colour excess is smaller than $E(B-V)$, at given A_V interstellar extinction, no attempt was made to correct $(V-I)_C$ for reddening. For emission line variables (suffix e), S stars, or for long-period variables with only one spectrum available, $\sigma_{(V-I)_C}$ = 1.20 mag was adopted.

Table 1.3.11. $(V-I)_C$ versus M sub-type for long-period variables

Type	$(V-I)_C$	$\sigma_{(V-I)}$	Type	$(V-I)_C$	$\sigma_{(V-I)}$	Type	$(V-I)_C$	$\sigma_{(V-I)}$
K5.5	1.61	0.14	M3	2.25	0.30	M6.5	4.32	0.80
M0	1.68	0.15	M3.5	2.40	0.37	M7	4.66	0.80
M0.5	1.76	0.16	M4	2.59	0.50	M7.5	5.03	0.80
M1	1.84	0.17	M4.5	2.91	0.75	M8	5.38	0.80
M1.5	1.94	0.18	M5	3.25	0.83	M8.5	5.75	0.80
M2	2.02	0.21	M5.5	3.61	0.82	M9	6.12	0.80
M2.5	2.13	0.22	M6	3.96	0.80	M10	6.80	1.20
Md	2.91	1.20	Me	3.00	1.20			

Stars without Colour, etc. (R–T)

Field H42 = R: When stars had no satellite colours nor photoelectric data, but an approximate V magnitude and a spectral type, and possibly a luminosity class, the intrinsic $(B-V)_J$ was derived from the spectral type. The reddened $(B-V)_J$ was estimated through a model galactic interstellar extinction, as a function of galactic coordinates and distance from the Sun (F. Arenou *et al.*, 1992, *Astronomy & Astrophysics*, 258, 104–111).

The $(V-I)_C$ was then deduced as in the case of genuine Johnson UBV data (method H), unless the stars are very red, reddened or of type M, R, S, N or C. For such stars the procedure was as for the photoelectric data (methods I to K).

Field H42 = S: When stars were reduced to the standard Hp system with an erroneous $(V-I)_C$ colour, the chromatic magnitude change, due to the irradiation of the optics in the space, was not adequately corrected. The resulting linear drift of magnitude could be used to recompute the true $(V-I)_C$. When the discrepancy was large and the stars non variable, the following relation was applied, where dHp/dt is the derivative of Hp, in magnitudes per day:

$$(V-I)_{new} = (V-I)_{old} - 1.429 \times 10^4 \, dHp/dt$$

Field H42 = T: This flag is used to signify stars with unknown colours reduced with $(V-I)_C = 0.666$ mag (Field H75), and also indicates entries where the final $V-I$ index was left blank. The latter was adopted when the final σ_{V-I} exceeded 0.25 mag for entries with $V-I < 1.5$ mag; the $(V-I)$ indices for redder stars, in particular long-period variables, are intrinsically inaccurate and were therefore retained in the catalogue independent of their associated errors (see Field H40).

Statistics

The number of entries in each of these categories is as follows:

H42	No.	H42	No.
A	2829	K	823
B	175	L	74269
C	1048	M	34
D	32	N	20
E	730	O	2631
F	455	P	13
G	209	Q	76
H	28369	R	1477
I	3170	S	177
J	406	T	1275